On Rayleigh and Fanno flows of homogeneous equilibrium two-phase fluids

S. K. Chan
School of Mechanical and Production Engineering, Nanyang Technological University, Singapore

W. A. Woods
Department of Mechanical Engineering, Queen Mary and Westfield College, University of London, London, UK

This article introduces a model fluid that has ideal liquid and perfect gas phases and a homogeneous two-phase mixture region. The thermodynamic-state properties of the model compare favorably with those of three common fluids.

A gas dynamic study of Rayleigh and Fanno flows is discussed using one approach similar to the classical work of Shercliff and another based on the proposed model.

The role of the isentropic and Newtonian and other new "sound speeds" are discussed. The relevance of these sound speeds in relation to critical speeds of the fluid is examined. It is concluded that in the two-phase region, a Rayleigh flow exhibits a maximum enthalpy at a point where the flow velocity reaches the isenthalpic speed of sound. This third speed of sound a_h is defined by the relation $a_h^2 = (\partial p/\partial \rho)_h$.

Keywords: homogeneous equilibrium two-phase; Rayleigh; Fanno; critical speeds

Introduction

There are many situations in which a one-dimensional (1-D) model gives a useful description of an actual flow. In most of these, the fluid is modeled as an incompressible liquid or perfect gas. A very successful example of the latter is the flow through a convergent–divergent nozzle. These models have been refined where needed, first, to take account of three-dimensional (3-D) effects and, secondly, to accommodate departures from ideal fluids.

The present article reports the results of a study of 1-D flows of a nonideal fluid. The state of the fluid can range from an incompressible liquid through a two-phase, liquid vapour region to a gaseous region.

The objectives of the article are, first, to present the ideas for a model fluid and to demonstrate that its resultant thermodynamic properties are reasonable; and secondly, to describe and discuss a study of Rayleigh and Fanno flows for homogeneous nonideal fluids, including a liquid–vapor two-phase mixture.

The goals of the article are to provide further understanding of Rayleigh and Fanno flows and the role of some new "speeds of sound," particularly the third or isenthalpic speed of sound,

$$a_h = \left(\frac{\partial p}{\partial \rho}\right)_h^{1/2}$$

Address reprint requests to Prof. Woods at Department of Mechanical Engineering, Queen Mary and Westfield College, University of London, Mile End Road, London E1 4NS, UK.

Received 29 April 1991; accepted 20 January 1992

This is in addition to the roles of the well-known isentropic and Newtonian sound speeds.

One-dimensional, steady-flow gas dynamics based on the perfect gas law for the case of a single-phase homogeneous fluid has been the subject of study in the past by many authors, in particular Shapiro and Hawthorne (1947). Such studies easily progress to simple analyses and establish the fact that the speed of sound is a critical velocity for nozzle flows, and for the Rayleigh and Fanno flows, whatever the fluid. In the case of an isothermal compressible flow, the critical speed is attributed to the so-called Newtonian sound speed. Books on the subject of compressible flows based on the perfect gas law are well established, e.g., Shapiro (1953) and Liepmann and Roshko (1957). Shercliff (1957/1958) has made a rigorous study of generalized steady 1-D flow, based on the fact that the state at each section of the flow in a strictly 1-D dynamical process can be uniquely described by three independent properties. With this assumption, Shercliff (1958) presented unique Maxwell-type relationships of the properties of the flow. The study also established the important roles of the speeds of adiabatic and Newtonian sound.

An example of a compressible, high-speed flow in a two-phase fluid can be found in the capillary tube of a refrigeration system, where high-pressure fluid expands adiabatically to a lower pressure. In this process, the fluid usually enters the tube saturated at a high pressure but leaves the tube as a mixture of liquid and vapor (ASHRAE Equipment Handbook, 1988). The fluid velocity at the exit can be high, and such a situation can be described as a two-phase Fanno flow (Stoecker and Jones, 1982).

In this article, an attempt is made to study flows in a duct in which the area does not change along the duct's length and

© 1992 Butterworth–Heinemann

in which the fluid remains in the two-phase state. A simple model of a two-phase fluid is used in which the fluid is assumed to be a homogeneous mixture of an ideal liquid and an ideal vapor, the proportion of which is given by the dryness fraction. An ideal liquid is, in this case, conveniently defined as one whose density and specific heat capacity do not change for the processes under consideration. An ideal vapor is defined as one obeying the perfect gas law. The model is then used to predict the behavior of Rayleigh and Fanno flows in a homogeneous two-phase region. In this work, considerations of slip between the phases and phase-change relaxation times are excluded.

Model for an ideal fluid

The liquid region

In the liquid region, an ideal liquid can be defined as one whose density ρ_o (or specific volume v_o) is a constant. For the model liquid, the value of v_o is selected as $0.4v^*$; this appears in Figure 1 as a straight line at $V_f = 0.4$. This assumption is not very accurate for liquids at high temperatures near the critical point. However, in most parts of the region of interest, the assumption of incompressibility can be shown to be reasonable. Data taken from Reynolds (1979) and given nondimensionally in Figure 1 show the saturated-liquid specific volume V_f against the saturated temperature θ_{sat} for water, refrigerant-22, and ammonia; it also shows that V_f does not change extensively over the range of interest. Both V_f and θ_{sat} are normalized using the thermodynamic critical-point values. Also, in the liquid region, it is assumed that the specific heat capacity c does not change with pressure and temperature. The values for c were taken from Rosenhow et al. (1985) corresponding to a temperature of 300 K.

As such, the equilibrium condition reduces to $Tds = cdT$, which, after integration, yields

$$\frac{s - s^*}{c} = \ln\left(\frac{T}{T^*}\right) \tag{1}$$

where the superscript (*) is used to denote properties at an

Notation

Lower-case letters

a_e	Speed of sound at constant internal energy
a_h	Isenthalpic speed of sound
a_S	Adiabatic speed of sound
a_T	Isothermal speed of sound
a_x	Speed of sound at constant dryness fraction

The above descriptions are intended to denote the expression $\left(\frac{\partial p}{\partial \rho}\right)_\phi^{1/2}$ where ϕ = e, h, s, T, or x

c	Specific heat capacity of liquid
c_p	Isobaric specific heat capacity of gas
c_v	Isochoric specific heat capacity of gas
e	Specific internal energy
h	Specific enthalpy
h_o	Specific stagnation enthalpy
k	Empirical nondimensional curve-fitting constant (Equations 9 and 11)
p	Pressure
s	Specific entropy
u	Velocity
v	Specific volume
v_o	Specific volume of ideal liquid
x	Dryness fraction

Upper-case letters

C	Empirical nondimensional parameter (Equation 11)
F	Impulse per unit area (Equation 17)
G	Mass velocity (Equation 18)
H	Nondimensional enthalpy (Equation 4)
M	Mach number
M_h	Isenthalpic Mach number
M_T	Isothermal or Newtonian Mach number
M_e	Iso-internal enogetic Mach number
P	Nondimensional pressure (Equation 3)
P_{sat}	Nondimensional saturation pressure
R	Characteristic gas constant
S	Nondimensional entropy (Equation 4)
T	Thermodynamic temperature
V	Nondimensional volume
V_o	$= \frac{v_o}{v^*} = 0.4$ nondimensional value for ideal liquid

Greek symbols

α	Nondimensional parameter (Equation 3)
β	Nondimensional parameter (Equation 29)
γ	Ratio of specific heat capacities, c_p/c_v
λ	Non-dimensional parameter (Equation 39)
ϕ	Variable to represent e, h, s, T, x
ρ	Density
ρ_o	Density of ideal liquid
θ	Nondimensional temperature (Equation 3)
θ_{sat}	Nondimensional saturation temperature

Superscript

*	Reference conditions

Subscripts

e	At constant internal energy
FAN	Along a Fanno curve
f	Saturated liquid conditions
g	Saturated vapor conditions
h	At constant enthalpy
o	Stagnation conditions also used to denote the specific and nondimensional volume of the ideal liquid when used with v and V, respectively
RAY	Along a Rayleigh curve
s	Isentropic conditions
sat	Saturation conditions
T	Isothermal conditions
x	At constant dryness fraction

Special symbol

^	Denotes the conditions at a prescribed location in the duct

arbitrary reference point. In this article, the reference condition used is the thermodynamic critical point unless otherwise stated. The change of the specific enthalpy is given by

$$h - h^* = c(T - T^*) + v^*(p - p^*) \tag{2}$$

By defining the nondimensional schemes

$$\theta = \frac{T}{T^*} \qquad P = \frac{p}{p^*} \qquad \alpha = \frac{v^*p^*}{cT^*} \tag{3}$$

$$S = \frac{s - s^*}{c} \qquad H = \frac{h - h^*}{cT^*} \tag{4}$$

Equations 1 and 2 can be written as

$$S = \ln(\theta) \tag{5}$$

$$H = (\theta - 1) + \alpha(P - 1) \tag{6}$$

We note that $(\partial H/\partial S)_P = \theta = e^S$ and $(\partial H/\partial P)_s = \alpha$, i.e., the distance between any two isobars in the enthalpy–entropy (H, S) thermodynamic plane along a line of fixed entropy is proportional to the pressure difference. Furthermore, this separation does not change with a change in the line of fixed entropy. The parameter α is expected to be small, of the order of 0.025, so the dependence of H on pressure P is small. Equations 5 and 6 are also assumed to apply at the saturated-liquid state, so the changes of specific entropy S_f and of enthalpy H_f are given by

$$S_f = \ln \theta_{sat} \tag{7}$$

and

$$H_f = (\theta_{sat} - 1) + \alpha(P_{sat} - 1) \tag{8}$$

In the two-phase region, pressure and temperature are dependent on each other, and an empirical relation between the saturated pressure P_{sat} and saturated temperature θ_{sat} is required. Figure 2 shows the variation of P_{sat} against θ_{sat} for water, refrigerant-22, and ammonia, and a suitable equation to represent the real fluid data adequately is given by

$$P_{sat} = (\theta_{sat})^k, \tag{9}$$

where k is a constant used for curve fitting. The magnitudes of this and of the other parameters used for calculating the curves for the model and the points for the actual fluids are given in Tables 1 and 2.

Figures 3 and 4 show the graphical representations of Equations 7 and 8 for the variations of S_f and H_f with saturated temperature θ_{sat}. Comparisons are made between the fluid properties for water, refrigerant-22, ammonia, and the model,

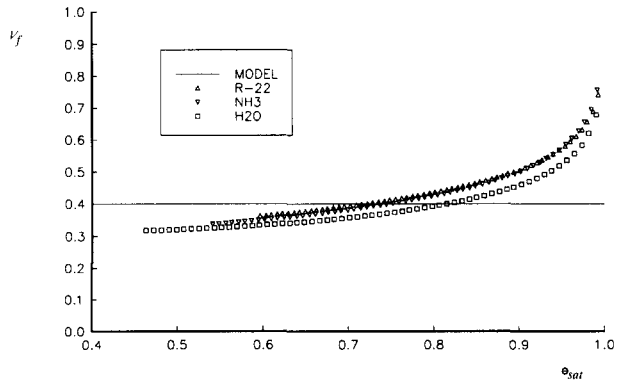

Figure 1 The variation of the normalized saturated-liquid specific volume with the normalized saturated temperature

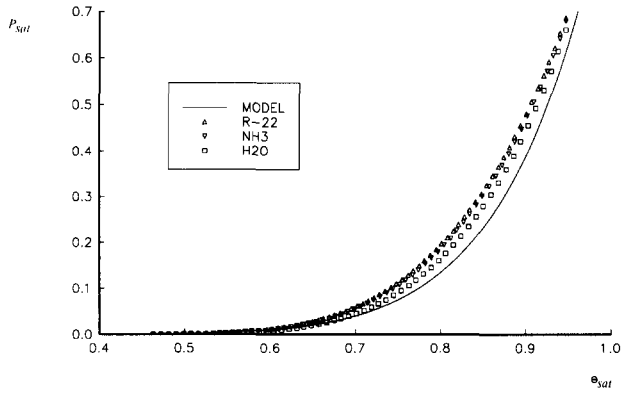

Figure 2 The variation of the normalized saturated pressure with the normalized saturated temperature

and they indicate that the model equations give reasonable representation of the real fluids.

The vapor region

In the vapor region, a perfect gas model is used. This is defined by the equation of state, $p = \rho RT$, together with the condition that the specific heat capacities do not change with temperature and pressure. As an approximation, the saturated-vapor state is also assumed to follow this law, so the specific volume, v_g, is given by $v_g = RT_{sat}/P_{sat}$ or, in the normalized form,

$$V_g = \frac{v_g}{v^*} = \left(\frac{RT^*}{v^*p^*}\right)\frac{\theta_{sat}}{P_{sat}} \tag{10}$$

where the term within the parentheses does not change for a given fluid, i.e.,

$$C = \frac{RT^*}{v^*p^*}$$

The values of R were taken from Reynolds (1979).

Equation 10 implies that V_g is a function of θ_{sat} (or P_{sat}) only. Figure 5 shows that the variation of V_g with saturated temperature, θ_{sat}, in the region of interest, except in the vicinity of the thermodynamic critical point, can be represented adequately by the equation

$$V_g = C(\theta_{sat})^{1-k} \tag{11}$$

The values of the dimensional empirical quantities and parameters for the selected fluids are summarized in Table 1, and the values of the nondimensional curve-fitting constant k and parameter C are given in Table 2. These values of C are approximately four, rather than the value of unity, which would satisfy Equation 11 at the thermodynamic critical point. However, to provide a reasonable fit for Figure 5, a compromise value of $C = 2$ has been used. This gives rise to discrepancies in x, which are most pronounced in the vicinity of the thermodynamic critical point, apparent later in Figures 8 and 11.

The two-phase homogeneous mixture region

The saturated mixture of the two-phase region can then be assumed to consist of a mixture of the ideal liquid, as already defined, and an ideal gas, the proportion of each phase being expressed in terms of the *dryness fraction*, x, which is defined as the ratio of the mass of the vapor component to the total

Table 1 Selected dimensional and nondimensional quantities and parameters[a]

	Dimensional quantities		
	Water	Refrigerant-22	Ammonia
T^* (K)	647.29	369.17	406.80
p^* (MPa)	22.089	4.9776	11.627
v^* (m^3/kg)	0.003155	0.001906	0.004208
h^* (kJ/kg)	2098.8	246.26	1233.56
s^* (kJ/kg K)	4.4289	0.8263	3.9069
R (J/kg K)	461.51	96.1467	488.21
c (J/kg K)	4179	1256	4810
Rayleigh G, kg/(m^2 s)	45830	27990	28791
Fanno G, kg/(m^2 s)	16485	11298	10512

Nondimensional quantities

$$\alpha = \frac{v^*p^*}{cT^*} = 0.025$$

$$C = \frac{RT^*}{v^*p^*} = 2.0$$

$$\lambda = \frac{G^2v^{*2}}{2cT^{*2}} = 0.0005$$

$$\beta = \frac{G^2v^{*2}}{p^*}$$

[a] Used in conjunction with the Reynolds Thermodynamic Properties (Reynolds 1979) in calculating the points shown on the figures. Note that the asterisk (*) refers to the thermodynamic critical point.

Table 2 Nondimensional parameters[a]

Magnitudes used in calculating the curves for the model shown in the figures	Magnitudes corresponding to actual property values		
	Water	Refrigerant-22	Ammonia
$\alpha = \frac{v^*p^*}{cT^*}$ 0.025	0.0258	0.0205	0.0250
$C = \frac{RT^*}{v^*p^*}$ 2.0	4.2865	3.7413	4.0592
$k = 9$			
$\lambda = \frac{G^2v^{*2}}{2cT^*}$ 0.0005			
$\beta = \frac{G^2v^{*2}}{p^*}$ 0.3			
$V_0 = \frac{v_0}{v^*}$ 0.4			

[a] Used in conjunction with the model fluid in calculating the curves shown on the figures. Note that the asterisk (*) refers to the thermodynamic critical point.

mass and is given by the equation

$$v = xv_g + (1 - x)v_f$$

or, in the normalized form,

$$V = V_f + x(V_g - V_f) \tag{12}$$

where $V = v/v^*$ and $V_f = v_f/v^*$. For the model liquid, we may put $V_f = 1$. We note that the thermodynamic critical point is a singularity and that at this point the dryness fraction x is indeterminate.

The link between the entropy value of the saturated vapor S_g and that of the saturated liquid S_f is provided by the Clausius–Clapeyron equation as

$$S_g = S_f + \alpha(V_g - V_f)\left(\frac{dP}{d\theta}\right)_{sat} \tag{13}$$

The saturated-vapor specific enthalpy H_g is given by

$$H_g = H_f + \theta_{sat}(S_g - S_f) \tag{14}$$

The specific entropy S and enthalpy H for the two-phase mixture region can be written in terms of their respective values at the saturated states and the dryness fraction as follows:

$$S = S_f + x(S_g - S_f) \tag{15}$$

$$H = H_f + x(H_g - H_f) \tag{16}$$

As mentioned above in connection with Equation 12, the dryness fraction is indeterminate at the thermodynamic critical

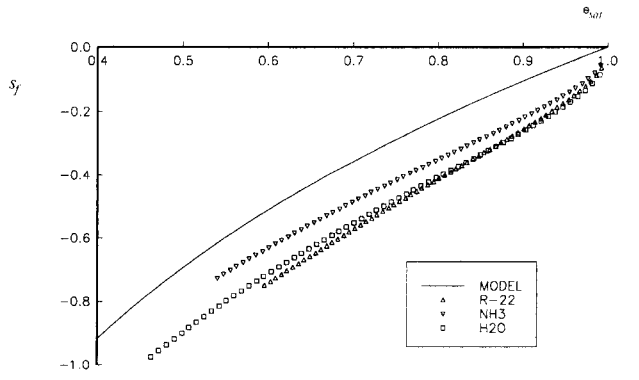

Figure 3 The variation of the normalized saturated-liquid specific entropy with the normalized saturated temperature

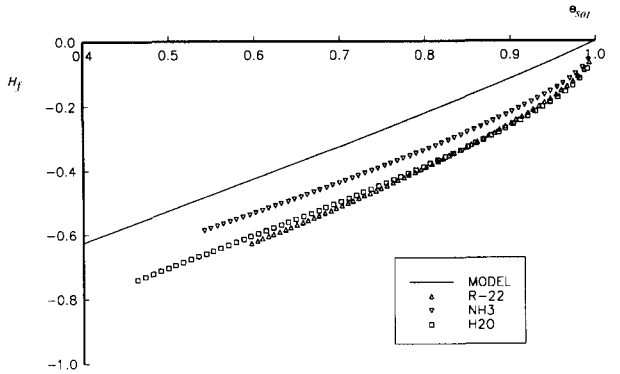

Figure 4 The variation of the normalized saturated-liquid specific enthalpy with the normalized saturated temperature

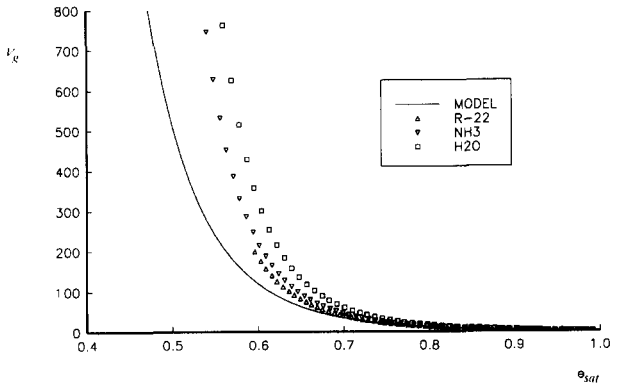

Figure 5 The variation of the normalized saturated-vapor specific volume with the normalized saturated temperature

point and the same difficulties occur in relation to the evaluation of x from Equations 15 and 16. This is almost certainly the explanation for the differences shown later between the model curve and the fluid data points at high pressures in Figures 8 and 11.

Rayleigh process

The Rayleigh process describes a steady, frictionless flow of fluid with heat transfer in a duct in which the cross-sectional area does not change along its length. The flow is characterized by the fact that the impulse per unit area F and the mass flow per unit area G also do not change along the length of the duct. Thus,

$$F = p + \rho u^2 = \hat{p} + \hat{\rho}\hat{u}^2 \tag{17}$$

and

$$G = \rho u = \hat{\rho}\hat{u} \tag{18}$$

where p is the pressure, ρ is the density, and u is the velocity. The symbol $\hat{}$ denotes the conditions at a prescribed location in the duct.

When Equations 17 and 18 are combined, we have $F = p + Gu$ so that $(\partial p/\partial u)_{\text{RAY}} = -G$ (the subscript $_{\text{RAY}}$ is to indicate that the differentiation is performed while keeping F and G unchanged). Hence, in an accelerating flow, p must necessarily decrease. For flow in the two-phase region, the temperature T must also decrease when u increases. Elimination of u from Equations 17 and 18 gives the equation

$$F = p + \frac{G^2}{\rho} \tag{19}$$

which describes the Rayleigh process as a family of curves (depending on the chosen values of F and G) in the plane of thermodynamic properties p and ρ.

The process can be represented in the plane of any two thermodynamic properties, such as the (ϕ, s) plane, where ϕ represents the thermodynamic property h, e, or T. Differentiation of Equation 19 yields

$$\left(\frac{\partial p}{\partial \rho}\right)_{\text{RAY}} = u^2 = M^2\left(\frac{\partial p}{\partial \rho}\right)_s \tag{20}$$

where M is the Mach number. By writing Equation 20 as

$$\left(\frac{\partial p}{\partial s}\right)_{\text{RAY}}\left(\frac{\partial \phi}{\partial p}\right)_s = M^2\left(\frac{\partial \rho}{\partial s}\right)_{\text{RAY}}\left(\frac{\partial \phi}{\partial \rho}\right)_s$$

we obtain

$$\left(\frac{\partial \phi}{\partial s}\right)_{\text{RAY}} - \left(\frac{\partial \phi}{\partial s}\right)_p = M^2\left\{\left(\frac{\partial \phi}{\partial s}\right)_{\text{RAY}} - \left(\frac{\partial \phi}{\partial s}\right)_\rho\right\}$$

Therefore,

$$\left(\frac{\partial \phi}{\partial s}\right)_{\text{RAY}} = \frac{(\partial\phi/\partial s)_p}{1 - M^2}\left\{1 - M^2\frac{(\partial\phi/\partial s)_\rho}{(\partial\phi/\partial s)_p}\right\}$$

$$= \frac{(\partial\phi/\partial s)_p}{1 - M^2}\left\{1 - M^2\frac{(\partial p/\partial \rho)_s}{(\partial p/\partial \rho)_\phi}\right\}$$

i.e.,

$$\left(\frac{\partial \phi}{\partial s}\right)_{\text{RAY}} = \left(\frac{\partial \phi}{\partial s}\right)_p\left(\frac{1 - M_\phi^2}{1 - M^2}\right) \tag{21}$$

where

$$M_\phi = u/a_\phi, \qquad a_\phi = (\partial p/\partial \rho)_\phi^{1/2}$$

Equation 21 describes the slope of the Rayleigh line in the (ϕ, s) plane and shows that this characteristic is applicable to all real fluid flows. It indicates that the slope has two stationary values occurring at $M_\phi = 1$ and at $M = 1$ when ϕ and s are at the maximum, respectively. The stationary value occurring at maximum s is identified as that occurring when the velocity is equal to the adiabatic sound speed, a_s. However, the stationary value at maximum ϕ occurs when the local velocity is equal to a_ϕ.

The energy equation is given by

$$h_o = h + \tfrac{1}{2}u^2 \tag{22}$$

where h_o is the stagnation enthalpy. The variation of h_o corresponds to heat transfer to or from the fluid. From the equilibrium condition, $dh = Tds + vdp$, we obtain

$$dh_o = Tds + vdp + udu = Tds$$

Hence, $(\partial h_o/\partial s)_{\text{RAY}} = T$, i.e., the effect of heat transfer is to drive the flow towards Mach unity in the case of heating and away from Mach unity in the case of cooling. When $\phi = h$, Equation 21 becomes

$$\left(\frac{\partial h}{\partial s}\right)_{\text{RAY}} = T\left(\frac{1 - M_h^2}{1 - M^2}\right) \tag{23}$$

and the sound speed a_h can be shown to be related to the adiabatic sound speed a_s, as follows:

$$\frac{a_s^2}{a_h^2} = \frac{(\partial p/\partial \rho)_s}{(\partial p/\partial \rho)_h} = \frac{(\partial h/\partial s)_\rho}{(\partial h/\partial s)_p} = 1 + \frac{1}{\rho c_v}\left(\frac{\partial p}{\partial T}\right)_\rho$$

Hence, $a_h < a_s$, since $(\partial p/\partial T)_\rho$ is always positive. In the subsonic region of the flow, heating will cause the enthalpy h to rise until the sound speed a_h is reached; thereafter, the enthalpy decreases until Mach unity. Between the sound speed a_h and the adiabatic sound speed, heating results in the decrease of the enthalpy, h, and an increase in the flow kinetic energy. In the supersonic region, as the entropy decreases, the enthalpy decreases and the rate of decrease also decreases from an infinite value at the sonic point.

When $\phi = e$, Equation 21 becomes

$$\left(\frac{\partial e}{\partial s}\right)_{\text{RAY}} = \left[T - p\left(\frac{\partial T}{\partial p}\right)_s\right]\left(\frac{1 - M_e^2}{1 - M^2}\right) \tag{24}$$

a_e is the speed of sound at constant internal energy, and M_e is the corresponding Mach number. The sound speed a_e can be shown to be related to the adiabatic sound speed a_s as follows:

$$\frac{a_e^2}{a_s^2} = 1 - \frac{p}{T}\left(\frac{\partial T}{\partial p}\right)_s$$

Hence $a_e < a_s$, since $(\partial T/\partial p)_s$ is always positive.

When $\phi = T$, Equation 21 becomes

$$\left(\frac{\partial T}{\partial s}\right)_{\text{RAY}} = \frac{T}{c_p}\left(\frac{1 - M_T^2}{1 - M^2}\right) \tag{25}$$

where M_T is the "isothermal" Mach number, i.e., the ratio u/a_T, and where $a_T = (\partial p/\partial \rho)_T^{1/2}$ is the isothermal or Newtonian sound speed. The ratio M_T^2/M^2 is equal to the specific heat capacity ratio γ, since

$$\frac{a_s^2}{a_T^2} = \frac{(\partial p/\partial \rho)_s}{(\partial p/\partial \rho)_T} = \frac{(\partial s/\partial T)_p}{(\partial s/\partial T)_\rho} = \frac{c_p}{c_v} = \gamma$$

Equation 25 is applicable to all flows in single-phase fluids in equilibrium and indicates that the stationary values of the flow occur at $M_T = 1$ and at $M = 1$ when T and s are stationary, respectively. For flows in two-phase fluids, c_p and M_T are both infinite, so that, in the limit, Equation 25 becomes

$$\left(\frac{\partial T}{\partial s}\right)_{\text{RAY}} = -\frac{T}{c_v}\left(\frac{M^2}{1 - M^2}\right), \tag{26}$$

which indicates that only one stationary value exists for the Rayleigh line in the (T, s) plane when the flow occurs in the two-phase region. The stationary value occurs at maximum entropy.

When flow occurs in the two-phase region, heating results in a decrease of temperature in the flow direction when flow is initially subsonic and an increase in temperature when flow is initially supersonic. This is to be expected, since pressure decreases with accelerating flow and increases in decelerating flow.

The density ρ in terms of the dryness fraction x and the pressure p may be written as

$$d\rho = \left(\frac{\partial \rho}{\partial p}\right)_x dp + \left(\frac{\partial \rho}{\partial x}\right)_p dx$$

Substituting into Equation 20, this becomes, after some rearrangement,

$$\left(\frac{\partial p}{\partial x}\right)_{\text{RAY}} = \frac{u^2(\partial \rho/\partial x)_p}{1 - u^2(\partial p/\partial \rho)_x} \tag{27}$$

Thus, at the point of maximum dryness fraction, a stationary value exists where the flow velocity u is equal to a_x, where $a_x = (\partial p/\partial \rho)_x^{1/2}$. The critical value a_x may be conveniently called the sound speed at constant dryness fraction. Therefore, in a heating process, the effect of heat transfer is to increase the dryness fraction until the point where $u = a_x$ is reached. The implication here is that the heat transfer in this case is being utilized for the conversion of the state of a fluid fraction from liquid to vapor.

Consider a Rayleigh curve that passes through the thermodynamic critical-state point. From Equation 19, we may write

$$p + G^2 v = p^* + G^2 v^*$$

or

$$(P - 1) + \beta(V - 1) = 0 \tag{28}$$

where

$$\beta = \frac{G^2 v^*}{p^*} \tag{29}$$

and is a parameter that depends upon the value of G.

Equation 28 is an alternative, normalized version of Equation 19 and represents families of the Rayleigh line (depending on the chosen values of β) on the pressure–volume (P, V) thermodynamic plane.

In the case of flow in a two-phase fluid, the specific volume V is given by Equation 12, so Equation 28 can be written as

$$(P_{\text{sat}} - 1) + \beta(V_g - 1)_x = 0 \tag{30}$$

The value of G selected to compute the curves shown in Figures 6, 7, and 8 is given in Table 1, and the corresponding values of the nondimensional parameter β are given in Table 2.

Since $V_g = V_g(P_{\text{sat}})$, Equation 30 represents the Rayleigh line in the (P, x) plane for various values of β. The Rayleigh line in the (θ, S) plane will be of interest. This can be obtained by

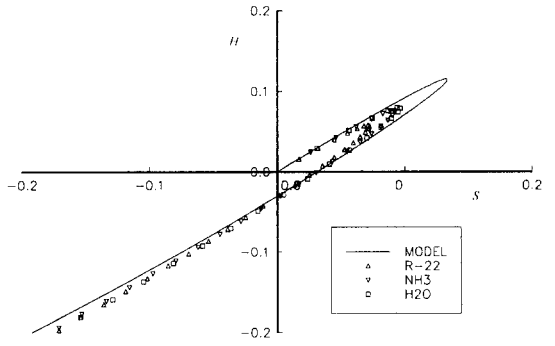

Figure 6 The Rayleigh process in the (H, S) thermodynamic plane for a homogeneous two-phase fluid

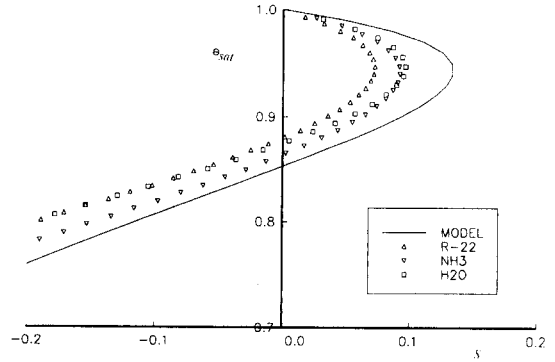

Figure 7 The Rayleigh process in the $(\theta_{sat}S)$ thermodynamic plane for a homogeneous two-phase fluid

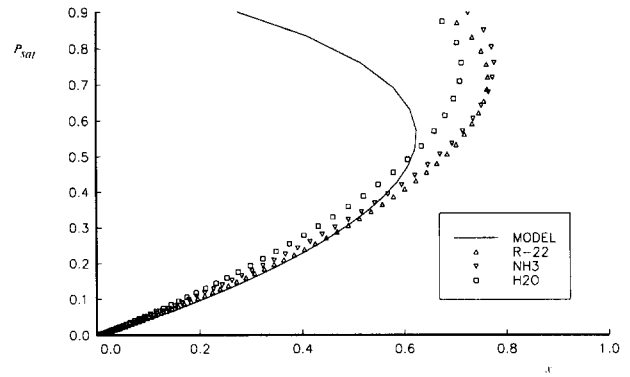

Figure 8 The Rayleigh process in the ($P_{sat} \sim x$) thermodynamic plane for a homogeneous two-phase fluid

combining Equations 15, 13, and 30, resulting in (after some rearrangement)

$$S = \ln \theta_{sat} + \left(\frac{\alpha}{\beta}\right)(1 - P_{sat})\left(\frac{dP}{d\theta}\right)_{sat} \tag{31}$$

By combining Equations 15, 16, and 14, we obtain

$$H = H_f + \theta_{sat}(S - S_f) \tag{32}$$

which, when combined with Equation 31, will result in the equation of the Rayleigh line in the enthalpy–entropy (H, S) plane. The comparisons shown in Figures 6, 7, and 8 are on the basis of the same values of α, β, and C.

Fanno process

The Fanno process is one of steady, adiabatic flow with friction in a duct in which the cross-sectional area does not change along its length. The friction leads to a force on the fluid in the opposite direction to the flow.

In a Fanno flow, the stagnation enthalpy h_o and mass flow per unit area G do not change along the duct. From Equations 18 and 22, we may write

$$h_o = h + \tfrac{1}{2}u^2 = h + \frac{G^2}{2\rho^2} = \hat{h}_o \tag{33}$$

which is a description of the Fanno process in the plane of the thermodynamic properties, enthalpy h and density ρ. The gradient of the curve is given by

$$\left(\frac{\partial h}{\partial \rho}\right)_{FAN} = \frac{u^2}{\rho} = \frac{M^2}{\rho}\left(\frac{\partial p}{\partial \rho}\right)_s \tag{34}$$

where the subscript $_{FAN}$ indicates that the differentiation is taken while keeping h_o and G unchanged.

The slope of the Fanno curve in the (h, s) plane can be derived by writing

$$\rho\left(\frac{\partial h}{\partial s}\right)_{FAN}\left(\frac{\partial h}{\partial p}\right)_s = M^2\left(\frac{\partial \rho}{\partial s}\right)_{FAN}\left(\frac{\partial h}{\partial \rho}\right)_s = M^2\left\{\left(\frac{\partial h}{\partial s}\right)_{FAN}\left(\frac{\partial h}{\partial s}\right)_\rho\right\}$$

Therefore,

$$\left(\frac{\partial h}{\partial s}\right)_{FAN} = \left(\frac{M^2}{M^2 - 1}\right)\left(\frac{\partial h}{\partial s}\right)_\rho = \frac{TM_h^2}{M^2 - 1} \tag{35}$$

Equation 35 implies that the effect of friction in a Fanno flow is to drive the flow towards Mach unity, with enthalpy decreasing in the subsonic branch and increasing in the supersonic branch. A stationary point exists at Mach unity.

In the (T, s) plane, however, the gradient of the Fanno line can be obtained by writing

$$\left(\frac{\partial T}{\partial s}\right)_{FAN} = \left(\frac{\partial h}{\partial s}\right)_{FAN}\left(\frac{\partial T}{\partial h}\right)_{FAN} = \left\{\left(\frac{\partial h}{\partial s}\right)_{FAN} - \left(\frac{\partial h}{\partial s}\right)_T\right\}\Big/\left(\frac{\partial h}{\partial T}\right)_s$$

where

$$\left(\frac{\partial h}{\partial s}\right)_T = T + \frac{1}{\rho}\left(\frac{\partial p}{\partial s}\right)_T$$

and

$$\left(\frac{\partial h}{\partial T}\right)_s = \frac{1}{\rho}\left(\frac{\partial p}{\partial T}\right)_s$$

Therefore,

$$\left(\frac{\partial T}{\partial s}\right)_{FAN} = \rho T\left(\frac{\partial T}{\partial p}\right)_s\left\{\frac{M_h^2}{M^2 - 1} - \frac{1}{\rho T}\left(\frac{\partial p}{\partial s}\right)_T - 1\right\} \tag{36}$$

For flow in the two-phase region, Equation 36 reduces to

$$\left(\frac{\partial T}{\partial s}\right)_{FAN} = \frac{\rho T}{(dp/dT)_{sat}}\left(\frac{M_h^2}{M^2 - 1} - 1\right) \tag{37}$$

which indicates that the flow reaches its maximum entropy when the Mach number is unity.

There is no stationary value at maximum T, since $M < M_h$. From Equation 33, since the stagnation enthalpy is fixed and for a Fanno curve that passed through the thermodynamic critical-state point, we may write

$$h + \tfrac{1}{2}G^2v^2 = h^* + \tfrac{1}{2}G^2v^{*2}$$

or

$$H + \lambda(V^2 - 1) = 0 \tag{38}$$

where

$$\lambda = \frac{G^2v^{*2}}{2cT^*} \tag{39}$$

The value of G selected to compute the curves shown in Figures 9, 10, and 11 is given in Table 1, and the corresponding values of the nondimensional parameter λ are given in Table 2.

Equation 38 provides an alternative version of Equation 33 that describes the Fanno process in the (H, V) plane for flows in all phases. The single parameter λ accounts for the mass velocity term, which could be varied. From Equations 7, 12, 13, and 15, it can be shown that

$$V = 1 + \frac{S - \ln(\theta_{sat})}{\alpha(dP/d\theta)_{sat}} \tag{40}$$

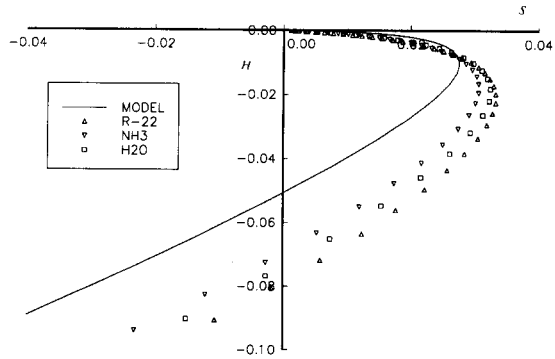

Figure 9 The Fanno process in the (H, S) thermodynamic plane for a homogeneous two-phase fluid

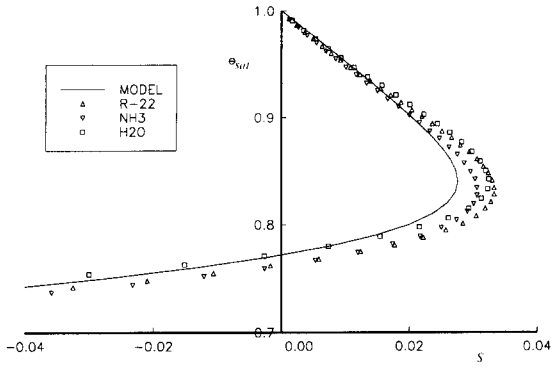

Figure 10 The Fanno process in the $(\theta_{sat}S)$ thermodynamic plane for a homogeneous two-phase fluid

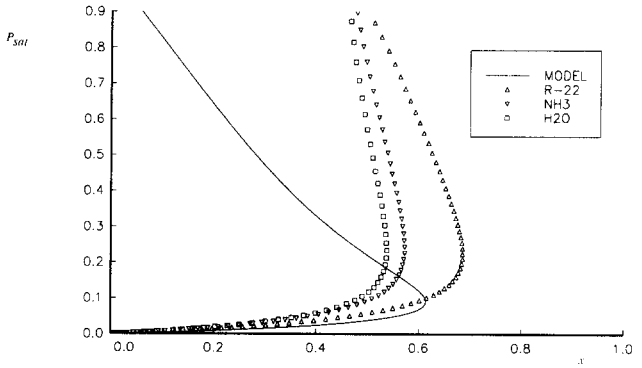

Figure 11 The Fanno process in the $(P_{sat}x)$ thermodynamic plane for a homogeneous two-phase fluid

Substitution of H (from Equation 32) and V (from Equation 40) into Equation 38 results in the equation of the Fanno line in the (θ, S) plane, i.e.,

$$(\theta_{sat} - 1) + \alpha(P_{sat} - 1) + \theta_{sat}(S - \ln \theta_{sat}) + \lambda\left\{\left(1 + \frac{S - \ln \theta_{sat}}{\alpha(dP/d\theta)_{sat}}\right)^2 - 1\right\} = 0 \qquad (41)$$

The corresponding equation of the Fanno line in the (H, S) plane can be obtained by eliminating θ_{sat} from Equations 32 and 41. The comparisons shown in Figures 9, 10, and 11 are on the basis of the same values of α, C, and λ.

Discussion

This section of this article is in two parts. The first discusses two aspects of the nondimensional parameters used for presenting the information on the figures. The first aspect considers how well the nondimensional parameters correlate the points for the three different fluids, and the second reviews how well the curves of the model represent the data points of the three actual fluids.

The second part of the discussion deals with the Rayleigh and Fanno flows and considers the nature of the flows and what they mean physically.

The correlation and representation aspects of the results

The first five diagrams give the static fluid properties. Figure 1 shows a very good correlation for R-22 and ammonia and quite a good correlation for water. The model is not good in the vicinity of the thermodynamic critical point and is fair elsewhere. Figure 2 shows a good correlation and a fair representation by the model. Figure 3 shows a very good correlation for R-22 and ammonia, with a fair one for water. There is a fair representation by the model, and this could be improved by the selection of a different value of c. Figure 4 shows a very good correlation for water and R-22, with quite a good one for ammonia. The model gives a fair representation and could be improved similarly to Figure 3, by the selection of a different c. Figure 5 shows a fair correlation for R-22 and ammonia, but not a very good one for water. The representation by the model is rather poor, and this could be improved by using a higher value, perhaps $C = 4$.

The next three figures are concerned with Rayleigh flows. Figure 6 shows a good correlation and quite a good representation by the model except in the vicinity of the sonic point. Figure 7 shows a fair correlation and the model gives a reasonable representation. Figure 8 shows a good correlation for R-22 and ammonia. The model gives a good representation for the lower half of the pressure range, but then deviates markedly. This point will be discussed again later.

The next three curves discuss the Fanno flows. At the critical point, Figure 9 shows a good correlation that deteriorates to fair as the enthalpy decreases. The model representation is similar, varying from good to poor as the enthalpy is decreased. Figure 10 shows a good correlation. The model gives a good representation except near the sonic point, where it is fair. In Figure 11, the parameters correlate the data points quite well for water and ammonia, but R-22 deviates quite markedly in the vicinity of maximum x. The model represents the trends quite well at low pressures, but then shows quite a different trend over most of the pressure range. The value of x is indeterminate at the critical point, and this will be discussed again later.

The nature and meaning of the Rayleigh and Fanno flows

Figures 6 and 7, respectively, show the variation of enthalpy H and saturated temperature θ_{sat} with entropy S for the Rayleigh process. The model fluid equations are used, and comparisons are made graphically using the properties of water, ammonia, and refrigerant-22. The general features of the graphs are similar and indicate the fact that the critical velocities of the fluids of the process occur, as predicted, when the enthalpy and entropy are at their maximum. It has been shown (Shercliff 1958) that for Rayleigh processes involving the perfect gas, the critical velocities of the fluids are associated with the points of maximum temperature and entropy. However, with flow occurring in a homogeneous two-phase fluid, where pressure and temperature are uniquely related properties, the isothermal speed of sound is always zero, since

$$\left(\frac{\partial p}{\partial \rho}\right)_T = 0.$$

Here, the point of maximum enthalpy occurs when the fluid velocity is equal to the speed

$$a_h = \left(\frac{\partial p}{\partial \rho}\right)_h^{1/2}$$

This is the speed at which infinitesimally small pressure

disturbances would travel if *the state changes within the disturbances occurred at constant enthalpy*. Because of this, a_h has been termed the isenthalpic speed of sound. On account of the analogy with

$$a_T = \left(\frac{\partial p}{\partial \rho}\right)_T^{1/2}$$

which is widely called the Newtonian speed of sound, it is reasonable to refer to a_h as the third speed of sound, thus implying that Newton's a_T is the second speed of sound. It is interesting to note that if the two-phase fluid is simplified to a single-phase gas, then the isenthalpic sound speed reduces to the Newtonian sound speed. Figure 7 shows that for a Rayleigh process, heat transfer in a subsonic accelerating flow leads to a decrease in temperature, which is the opposite effect to that for a gaseous flow accelerating below the Newtonian Mach number M_T. This is because the heat transfer is being used to increase the kinetic energy and to increase the vapor portion of the fluid stream. Figure 8 shows that the dryness fraction of the fluid increases as the pressure decreases in a subsonic accelerating flow. The differences apparent at high pressures are thought to be due to the indeterminacy of the dryness fraction at the thermodynamic critical point.

Figures 9, 10, and 11 show the behavior of the Fanno process in a two-phase flow. The process, as plotted in the (H, S) plane (Figure 9), is similar to that in the (θ, S) plane for a single-phase gaseous flow. The change of enthalpy in the subsonic branch of the flow is considered to be small, and it would be reasonable to assume that enthalpy remains essentially constant in many practical cases, such as flow in the expansion tube of a refrigeration system. However, temperature and pressure changes are significant in the subsonic branch of the process, as shown in Figure 10. The calculated results shown in Figure 11 indicate that the change in the dryness fraction in the subsonic branch of the process is quite small. The redistribution of energy required for the change of phase of the fluid from the liquid to the vapor state is the result of a friction-generated, combined temperature reduction and drying process. The change of the dryness fraction predicted by the model fluid is not particularly accurate at high pressures because of limitations imposed by the indeterminacy of the dryness fraction at the thermodynamic critical point already mentioned.

Conclusions

The parameters selected to present the results correlate the data for the three fluids quite well. The exceptions are the cases involving the dryness fraction in the vicinity of the thermodynamic critical point.

The model fluid represents the trends quite well in most cases. The exceptions are those involving the dryness fraction in the vicinity of the thermodynamic critical point. There is also a slight deviation near the sonic point for Rayleigh and Fanno flows.

The results of the thermodynamic analyses have shown that the general behavior of the Rayleigh and Fanno processes, whatever the fluid, is qualitatively similar to that involving the perfect gas only, as demonstrated by Shercliff (1958). For flows involving saturated two-phase fluid only, the characteristics of the flows are governed by the pressure/temperature dependence, so in the case of an accelerating flow with pressure reducing, the temperature has to reduce but enthalpy and internal energy may increase or decrease. The latent heat of vaporization, needed to increase the dryness fraction of the fluid for an accelerating flow, is derived from the heat transfer to the fluid in the case of the Rayleigh process, and is generated as a result of frictional dissipation in the case of the Fanno process.

The significance of adiabatic and Newtonian sound speeds in single-phase gaseous flows have been demonstrated by Shercliff (1958).

In Rayleigh flows in two-phase fluids, a point of maximum enthalpy occurs where the flow velocity reaches the isenthalpic "speed of sound." This has become the significant parameter for two-phase fluids. For the perfect gas flow, the isenthalpic sound speed degenerates to that of the isothermal sound speed, i.e., Newtonian sound speed. Hence the isenthalpic speed of sound could be considered to be more general than the Newtonian speed of sound.

A simple model of a homogeneous two-phase fluid has been presented. It has been shown to be capable of predicting satisfactorily the general features of the Rayleigh and Fanno flows in a two-phase fluid environment.

References

ASHRAE Equipment Handbook. (1988) Chapter 19, p. 22

Liepmann, H. W. and Roshko, A. (1957) *Elements of Gas Dynamics*. John Wiley and Sons, New York

Reynolds, W. C. (1979) *Thermodynamic Properties in S.I.* Department of Mechanical Engineering, Stanford University, Stanford, CA

Rosenhow, W. M., Hartnett, J. P., and Ganic, E. N. (1985) *Handbook of Heat Transfer Fundamentals*. McGraw-Hill, New York, Chapter 3

Shapiro, A. H. (1953) *The Dynamics and Thermodynamics of Compressible Fluid Flow*, Vol. 1. The Ronald Press Company, New York

Shapiro, A. H. and Hawthorne, W. R. (1947) The mechanics and thermodynamics of steady one-dimensional gas flow. *J. Appl. Mech.*, **14**, 317

Shercliff, J. A. (1958) Some generalizations in steady one-dimensional gas dynamics. *J. Fluid Mech.*, **3**, 645–657

Stocker, W. F. and Jones, J. W. (1982) *Refrigeration and Air-Conditioning*. second ed. McGraw Hill, New York